Proc. Natl. Acad. Sci. USA
Vol. 85, pp. 3628–3632, May 1988
Neurobiology

Neuroanatomical localization and quantification of amyloid precursor protein mRNA by *in situ* hybridization in the brains of normal, aneuploid, and lesioned mice

(gene expression/Down syndrome/Alzheimer disease)

CATERINA BENDOTTI, GIAN LUIGI FORLONI, RICHARD A. MORGAN, BRUCE F. O'HARA, MARY LOU OSTER-GRANITE, ROGER H. REEVES, JOHN D. GEARHART, AND JOSEPH T. COYLE*

The Johns Hopkins University School of Medicine, Baltimore, MD 21205

Communicated by Seymour S. Kety, December 24, 1987 (received for review September 17, 1987)

ABSTRACT **Amyloid precursor protein mRNA was localized in frozen sections from normal and experimentally lesioned adult mouse brain and from normal and aneuploid fetal mouse brain by *in situ* hybridization with a ^{35}S-labeled mouse cDNA probe. The highest levels of hybridization in adult brain were associated with neurons, primarily in telencephalic structures. The dense labeling associated with hippocampal pyramidal cells was reduced significantly when the cells were eliminated by injection of the neurotoxin ibotenic acid but was not affected when electrolytic lesions were placed in the medial septum. Since the gene encoding amyloid precursor protein has been localized to mouse chromosome 16, we also examined the expression of this gene in the brains of mouse embryos with trisomy 16 and trisomy 19 at 15 days of gestation. RNA gel blot analysis and *in situ* hybridization showed a marked increase in amyloid precursor protein mRNA in the trisomy 16 mouse head and brain when compared with euploid littermates or with trisomy 19 mice.**

Cerebrovascular A4 amyloid peptide has been identified as a major extracellular component of senile neuritic plaques and cerebrovascular amyloidosis, characteristic features of brain histopathology observed in individuals with Alzheimer disease (AD) and in individuals with Down syndrome (DS) with AD pathology (1–4). Investigators in several laboratories have used oligonucleotide probes corresponding to the amino acid sequence of the A4 peptide to isolate a cDNA clone corresponding to the amyloid precursor protein (5–7). The gene encoding the amyloid precursor protein has been mapped to human chromosome 21, suggesting it may be involved in the development of the pathologic stigmata of AD seen in virtually all individuals with DS surviving as adults (3, 4, 8–10).

Because genetic homology exists between human chromosome 21 and mouse chromosome 16 (10–13), mice with trisomy 16 (Ts16) provide a rodent model for studies relevant to DS. Neurochemical, neurophysiological, and neuroanatomical alterations reported for DS individuals have also been observed in the brains of Ts16 mice (8, 14). The genetic homology between human chromosome 21 and mouse chromosome 16 has been extended to include the gene encoding the mouse homologue of amyloid precursor protein (gene symbol, *App*) (12, 13). Thus, the Ts16 mouse may also provide an experimental model to examine the developmental consequences of increased levels of expression of *App*, as occurs in DS and possibly in AD (15). Accordingly, we have used a mouse cDNA clone as a probe to examine and quantify the distribution of App mRNA and to determine its cellular localization in the brains of normal adult mice and in the brains of normal and trisomic [Ts16 and trisomy 19 (Ts19)] mouse fetuses at 15 days of gestation (DG).

MATERIALS AND METHODS

Tissue Preparation. Adult C57BL/6J and BALB/cJ mice were anesthetized with Avertin, then perfused transcardially with isotonic phosphate-buffered saline (PBS), and then immediately perfused with 4% (wt/vol) paraformaldehyde in PBS. The brains were removed, postfixed for 2 hr at 4°C in fresh 4% (wt/vol) paraformaldehyde in PBS, and incubated overnight in 20% (wt/vol) sucrose in PBS for subsequent cryoprotection. The brains were then frozen rapidly in isopentane and dry ice. Ten-micrometer sections were cut with a cryostat, thaw-mounted onto slides coated with Denhardt's solution (0.02% polyvinylpyrrolidone/0.02% Ficoll/0.02% bovine serum albumin), and stored at −70°C.

Adult BALB/cJ mice, anesthetized with halothane (3%) and mounted in a stereotactic apparatus, received unilateral injections of ibotenic acid (5 μg in 0.5 μl of saline) into the hippocampal formation with a Hamilton microsyringe (16). Electrolytic lesion of the medial septum was used to remove cholinergic afferents to the hippocampus (17). The animals were allowed to recover for 7 days before transcardial perfusion as described above.

The Ts19 and Ts16 mouse fetuses were obtained by using a mating scheme described in detail in Gearhart *et al.* (18). At 15 DG (day of vaginal plug = 0 DG) fetuses were collected under Avertin anesthesia. Each fetus was perfused transcardially with 3 ml of 4% (wt/vol) paraformaldehyde in PBS, after removal of the liver for karyotype analysis (19). The heads were removed and processed as described above. The respective normal (2*N*) littermates were used as controls for the quantitative analysis of *App* expression in Ts16 and Ts19 embryos.

Probe Preparation. Molecular probes were prepared from a 1.0-kilobase *Eco*RI fragment of a mouse cDNA clone representing the A4 and proximal 3′-untranslated portion of the App mRNA (20). Probes were synthesized by primer extension (21). ^{35}S-labeling was accomplished by using the same procedure by substituting 30 μCi (1 Ci = 37 GBq) of adenosine 5′-[γ-[^{35}S]thio]triphosphate and cytidine 5′-[γ-[^{35}S]thio]triphosphate, producing probe fragments of 50–300 base pairs with a specific radioactivity >10^9 cpm/μg.

Hybridization Procedure. The hybridization procedure was based on the protocol of Young (22). Control slides were incubated in RNase A (50 μg/ml in 0.1 M sodium phosphate, pH 7.4) for 1 hr at 37°C, rinsed twice in 0.1 M sodium

The publication costs of this article were defrayed in part by page charge payment. This article must therefore be hereby marked "*advertisement*" in accordance with 18 U.S.C. §1734 solely to indicate this fact.

Abbreviations: *App*, amyloid precursor protein gene; AD, Alzheimer disease; DS, Down syndrome; Ts16, trisomy 16; Ts19, trisomy 19; DG, day(s) of gestation.

*To whom reprint requests should be addressed.

phosphate/0.15 M NaCl, and dehydrated prior to hybridization. For competition experiments, adjacent sections were prehybridized with 100-fold excess of gel-purified nonradioactive mouse App cDNA dissolved in prehybridization buffer containing 4× SSC (0.6 M NaCl/0.06 M sodium citrate, pH 7.0), 50% (vol/vol) deionized formamide, 10% (wt/vol) dextran sulfate, 1× Denhardt's solution, sheared single-stranded calf thymus DNA (1 mg/ml), yeast tRNA (1 mg/ml), and 10 mM dithiothreitol or in prehybridization buffer alone for 10 hr at 37°C. Sections were then rinsed for 1 hr in 1× SSC at 55°C and dehydrated. *In situ* hybridization was done in 20 ml of the same buffer plus 0.5×10^6 cpm of probe per section; the sections were covered with parafilm coverslips and incubated at 37°C for 16–20 hr.

The coverslips were removed in 1× SSC, and the sections were rinsed for 1 hr in 1× SSC at 55°C, followed by 1 hr in 1× SSC and 1 hr in 0.1× SSC, at room temperature. The slides were rinsed in deionized water, dried under an air stream, and exposed to Hyperfilm (Amersham) for autoradiography. Films were developed after 5–6 days, and the sections were dipped in NTB3 emulsion (Kodak, diluted 1:1 with water), exposed at 4°C for 6–10 days and then developed and stained with cresyl violet.

Analysis of Autoradiograms. Film autoradiograms were placed on a lightbox, illuminated with white light, and scanned for grain density with a computerized analysis system (RAS R-1000, Amersham). Visual display of the digitized image was color transformed and represented in an analogue scale as optical density (OD). Preliminary experiments with various exposure times established the linear response range of the calibration curve. The concentration used was determined empirically, based on the optimal signal to nonspecific background ratio obtained. A linear standard curve was generated from ^{35}S-labeled standards prepared with "brain paste" to correct for quenching of the radioactive signal (22), which allowed direct comparisons with the radiolabeled standard on the same film. Cresyl violet-stained sections dipped in photographic emulsion were analyzed for cellular localization of silver grains by bright-field illumination.

RNA Gel Blot Analysis. Total RNA was isolated from the heads of 15 DG mice (both Ts16 and euploid) as described by Chirgwin *et al.* (23). Ten micrograms of each RNA was then subjected to formaldehyde/gel electrophoresis, transferred to nylon membranes (Magna 66, MSI) (24), and fixed by UV cross-linking (25). Hybridization was as described by Melton *et al.* (26).

RESULTS

Expression of App mRNA in Mouse Brain. *In situ* hybridization with a ^{35}S-labeled cDNA clone homologous to the mouse *App* gene (20) on sections of adult mouse brain showed regional differences in the intensity of hybridization (Fig. 1*A*). Heavily labeled (OD > 0.60) nuclei or regions included the olfactory system, the frontal cortex, the pyramidal layer of the hippocampus, the area preopticum, and the internal granular and Purkinje cell layers (stratum granulosum) of the cerebellar cortex (Table 1). Whereas several brain regions were intermediate in value (OD = 0.60–0.30), lightly labeled (OD < 0.30) regions or nuclei included: the globus pallidus; molecular layer (stratum moleculare) of the cerebellar cortex; the strata moleculare, radiatum, and oriens of the hippocampus; pars reticulata of the substantia nigra; and the nucleus centralis pontis (Table 1). Treatment with RNase significantly reduced the signal of specific hybridization; however, in some areas, a nonspecific signal remained over the white matter (Fig. 1*A*). Prehybridization with excess unlabeled App cDNA also resulted in a marked attenuation (70–80%) of the highest hybridization densities (Fig. 1A).

Table 1. App mRNA hybridization densities over brain regions of adult mouse

Brain area	OD
Cortex	
Frontal	1.00 ± 0.12
Frontoparietal	0.64 ± 0.13
Area pyriformis	0.62 ± 0.15
Parietal	0.54 ± 0.13
Occipital	0.46 ± 0.10
Temporal	0.51 ± 0.10
Olfactory system	
N. olfactorius anterior	1.00 ± 0.12
Tuberculum olfactorius	0.73 ± 0.30
Septal region	
N. lateralis	0.44 ± 0.06
N. medialis	0.32 ± 0.07
Basal ganglia	
N. accumbens septi	0.51 ± 0.12
N. caudatoputamen	0.34 ± 0.13
Globus pallidus	0.17 ± 0.07
Hippocampus	
Dentate gyrus (granular layer)	0.46 ± 0.05
Hilus fasciae dentatus	0.41 ± 0.05
Pyramidal layer CA1	0.40 ± 0.07
Pyramidal layer CA2	0.61 ± 0.07
Pyramidal layer CA3	0.62 ± 0.03
Stratum oriens	0.23 ± 0.07
Stratum moleculare-radiatum	0.12 ± 0.03
Thalamus	
N. paraventricularis	0.47 ± 0.10
N. reticularis	0.35 ± 0.04
N. medialis	0.25 ± 0.04
Medial habenulae	0.50 ± 0.13
Mesencephalon	
Substantia nigra	
compacta	0.39 ± 0.11
reticularis	0.20 ± 0.06
N. interpeduncularis	0.47 ± 0.04
N. ventral tegmenti	0.52 ± 0.13
Colliculi	0.41 ± 0.02
Pons-medulla oblongata	
N. pontis	0.57 ± 0.05
Substantia grisea centralis pontis	0.44 ± 0.12
N. centralis pontis	0.22 ± 0.03
N. vestibularis	0.49 ± 0.02
Cerebellum	
Stratum moleculare	0.14 ± 0.03
Stratum granulosum	1.00 ± 0.16
N. lateralis	0.37 ± 0.03
Hypothalamus	
Area preoptica	0.71 ± 0.12
Area ventromedialis	0.34 ± 0.07
Area dorsolateralis	0.37 ± 0.06
N. mamillaris	0.39 ± 0.15

The values represent the mean ± SD of the OD of at least three analyses of each brain region examined.

Neuronal Localization of App mRNA. The cellular localization of the hybridization signal was examined microscopically on sections dipped in photographic emulsion. A dense pattern of labeling with silver grains was localized over cell bodies of the pyramidal neurons of the cerebral cortex and of the hippocampus and localized in the Purkinje and granule cells of the cerebellar cortex. Few silver grains were localized over glial cells, or in regions rich in glia, such as the globus pallidus and corpus callosum. In the brains of animals in which ibotenic acid lesion resulted in the elimination of hippocampal pyramidal cells in CA2 and CA3, the intense hybridization signal coinciding with the pyramidal cell so-

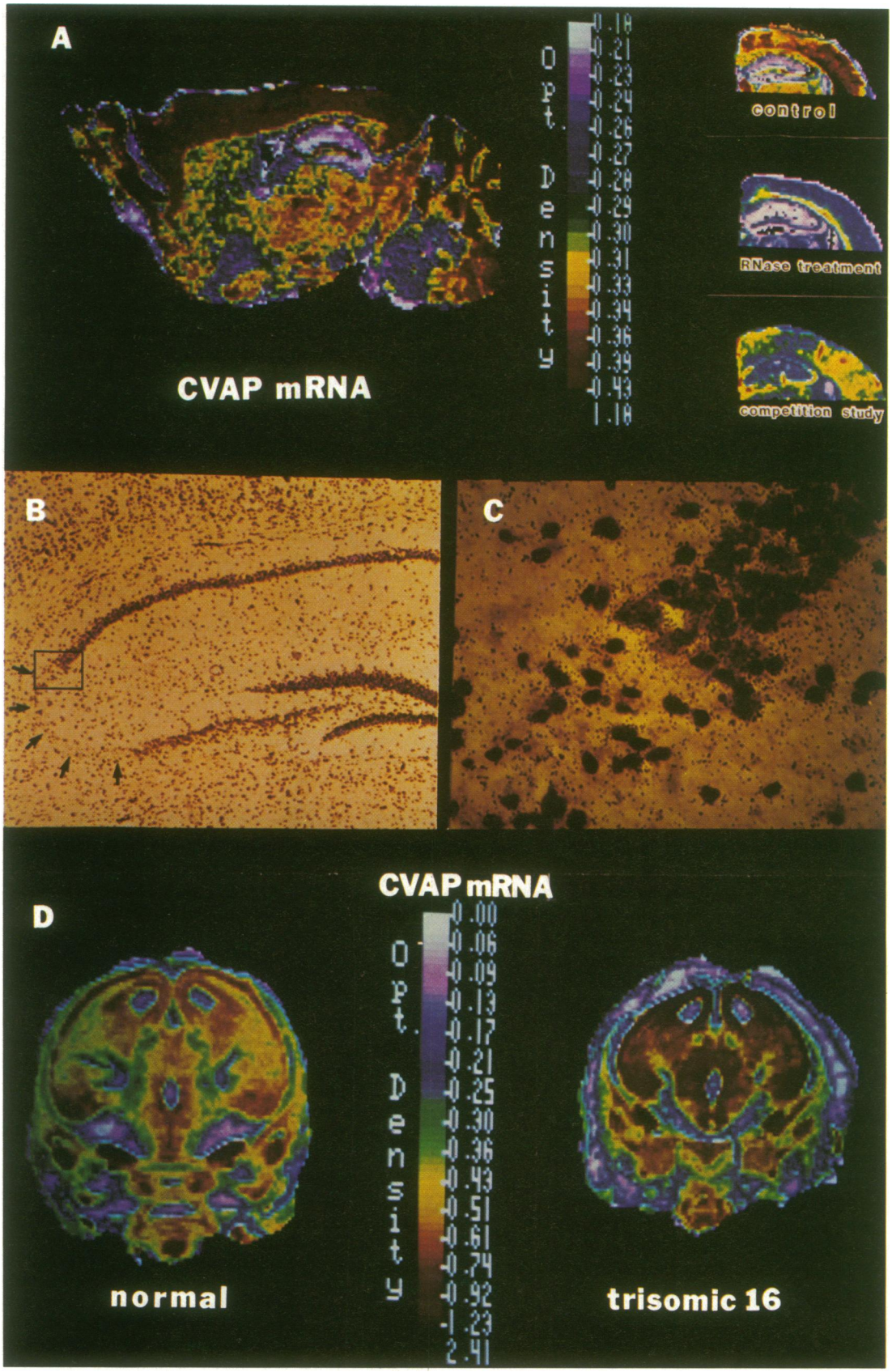

FIG. 1. Expression of App mRNA in mouse brain. (*A*) Color-enhanced computer image of parasagittal section of normal adult mouse brain hybridized with ^{35}S-labeled cDNA probe for mouse *App* on the left. CVAP, cerebrovascular A4 amyloid peptide. On the right are portions of coronal sections illustrating the cerebral cortex and hippocampal formation. The top section was taken from an untreated control adult mouse brain, the middle section was from an RNase-treated control, and the bottom section was from a competition study (excess unlabeled probe) control. Note that the OD measurements in this particular photograph range from 0.00 to 1.10, as they do in sections examined to generate data for Table 1. (*B*) Section hybridized with ^{35}S-labeled App cDNA probe and stained with cresyl violet. This section through Ammon's horn was obtained from a normal adult mouse that received injections of ibotenic acid in the dorsal and ventral hippocampus 7 days before the animal

mata was also eliminated (Fig. 1*C*). In contrast, electrolytic lesions of the medial septum, which cause a degeneration of hippocampal cholinergic afferents, did not affect perceptibly the autoradiographic distribution of App mRNA in the hippocampus ($n = 3$; data not illustrated).

Expression of App mRNA in Aneuploid Mouse Fetuses. In the brains of euploid fetuses at 15 DG, the highest densities of hybridization were localized to the neocortex, pyriform cortex, subventricular zone, and hypothalamus (Fig. 1*D*). Peripheral tissues, such as the trigeminal ganglia, sphenoidal bones and cartilages, and salivary glands also gave strong signals. In the heads of Ts16 fetuses, the distribution of App mRNA was similar to that of the normal littermates, but the intensity of the signal was clearly increased (Fig. 1*D*). Measurements made of whole brain sections indicated a 55% increase of signal ($P > 0.001$; two-tailed t test) in the Ts16 brain (OD = 0.34 ± 0.03; $n = 7$) compared with the normal littermate (OD = 0.22 ± 0.02; $n = 7$); however, some areas exhibited an even greater increase in the Ts16 brain.

RNA gel blot analysis of total RNA extracted from the heads of 15 DG fetuses confirmed the *in situ* hybridization results (Fig. 2). The level of App mRNA was clearly elevated in the heads of 15 DG Ts16 mice relative to the amount of RNA loaded (10 μg per sample) and to the amount of expression of the control β-actin gene; the size of the transcript was not changed (Fig. 2).

To determine whether increased *App* expression is specific to Ts16 or a general response to the aneuploid state, the hybridization pattern in the heads from Ts19 mice at 15 DG was examined. Ts19 mice exhibit significant retardation in neuronal development (14) and characteristic neurochemical abnormalities (27). No differences were observed ($P > 0.5$, two-tailed t test) in the levels of *App* expression in Ts19 fetal brains (OD = 0.24 ± 0.08; $n = 4$) when compared to normal littermates (OD = 0.23 ± 0.04; $n = 4$) (data not illustrated).

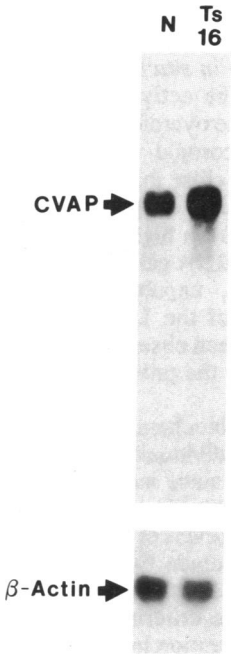

FIG. 2. RNA gel blot analysis of App mRNA. RNA (10 μg) isolated from the head of mice at 15 DG was subjected to formaldehyde/gel electrophoresis, transferred to nylon membranes, and hybridized with a mouse App probe. The arrow indicates the 3.3-kilobase App mRNA detected in both the euploid (2*N*) and trisomy 16 (Ts16) lanes. Below, as a control, the blot was subsequently stripped and reprobed with the β-actin gene probe.

DISCUSSION

In situ hybridization has been used to localize the expression of App mRNA regionally and at the cellular level in the mouse brain. The specificity of hybridization was demonstrated by the significant reduction of hybridization signal with prior RNase treatment of the section and after prehybridization with excess of unlabeled probe. The *App* gene appears to be transcribed preferentially in neurons, since the highest grain densities were clustered over the pyramidal neurons of the hippocampus and the cerebral cortex and over the Purkinje cells and granule cells in the cerebellum. In general, grain density over glial cells was sparse; and glial-enriched structures, such as the corpus callosum and globus pallidus, exhibited low density of labeling with the App probe. Nevertheless, this survey does not preclude the expression of *App* in glia and other nonneuronal elements. On the contrary, intense expression was observed in fetal nonneuronal tissues—such as the salivary glands, cartilages at the base of the skull, and bone. The localization of App mRNA in neurons was confirmed by ibotenic acid lesions of the hippocampal pyramidal neurons, which produced a striking focal reduction of the hybridization signal that coincided with the depletion of pyramidal cells in the CA2 and CA3 areas of Ammon's horn. In contrast, prior lesion of the medial septum, which removes cholinergic afferents to the hippocampus, did not affect the distribution of App mRNA in the hippocampus. This result suggests that *App* expression in pyramidal cells is not regulated by synaptic interactions with these cholinergic afferents, which are particularly vulnerable in AD and DS (3, 8).

Our findings on the distribution of App mRNA expression in the adult mouse brain are consistent with the *in situ* hybridization results of Bahmanyar *et al.* (28) in primate brain. They found that the highest densities of grains were clustered over the pyramidal neurons of CA1 and CA3 of Ammon's horn and over the pyramidal neurons of layer V of the superior frontal gyrus and layers III and V of areas 9 and 46. Oligodendrocytes and Purkinje cells of the cerebellum were also reported to exhibit high label density (28). The apparent discrepancy between our *in situ* hybridization results and those with RNA blot analyses of Tanzi *et al.* (29) in human brain likely reflects the fact that specific cell populations within particular regions, such as the cerebellum and hippocampus, express high levels of App mRNA, whereas the majority of cells in the region express only moderate to low levels of App mRNA.

Since *App* has been localized to mouse chromosome 16 (12, 13), it was of interest to examine the expression of this gene in Ts16 mice. mRNA levels were increased in Ts16 mice when compared to euploid littermates as judged by RNA gel blot analysis, with RNA from fetal heads, and by *in situ* hybridization. Since Ts16 in mice results in brain hypoplasia, we examined whether this increased expression was a consequence of increased gene dosage or simply a nonspecific consequence of aneuploidy on brain development. To distinguish between these possibilities, analyses were also conducted on Ts19 fetuses, which exhibit brain hypoplasia and impaired cerebral development, although the neuronal systems involved differ from those affected in Ts16 mice (14, 18, 27, 30). In Ts19 fetuses, *App* expression in brain at 15 DG was not different from that of euploid littermate controls or from the euploid littermate controls of the Ts16 mice.

was killed. Arrows indicate the area of destruction of pyramidal neurons in CA2-3 (×45). (*C*) Higher magnification (×450) of the boxed region in *B*. Note the density of grains over the pyramidal cells is much higher than the density of grains over the area where the pyramidal neurons were removed by lesion with ibotenic acid 7 days earlier. (*D*) Color-enhanced computer images of expression of App mRNA in the heads of normal (*Left*) and trisomy 16 (Ts16) (*Right*) mice at 15 DG. Note that the OD varies from 0.00 to 2.41. There is a clear increase in hybridization signal, but a similar distribution of expression in various brain regions of Ts16, relative to a control littermate fetal mouse brain.

RNA gel blot analysis demonstrated that App mRNA structure is not changed grossly in Ts16 mice. Thus, the increased grain density observed by *in situ* hybridization of Ts16 fetal heads was not due to the activation of a new *App*-like gene. Additionally, while the overall increase in OD measurements averaged 55% for coronal sections of the whole brain of Ts16 mouse fetuses, close inspection of Fig. 1*D* reveals that specific regions, such as portions of the developing cerebral cortices, have even higher grain densities, and densitometric scans of the RNA gel blots indicate a 2.5- to 3.0-fold increase (R.A.M., unpublished results). Levels of gene product in excess of the 1.5-fold increase expected in the trisomic state have been observed (10, 11, 14) in Ts16 mice and DS individuals for the products of several genes.

Ts16 mice possess a number of biochemical, structural, and functional similarities with DS individuals (8, 14, 30). Our findings extend these observations, since increased expression of the *App* gene has been observed in the brains of DS fetuses at week 19 of gestation (29). Levels of the App mRNA may be elevated much earlier in human beings, since the developmental stage that we examined in the mouse (15 DG) corresponds by overall morphologic criteria to a developmental stage of ≈60 days after conception in human beings.

The concurrent localization of App mRNA and the identification and localization of the amyloid protein product by immunocytochemistry in an animal model of DS could be useful in attempting to identify factors involved in the early stages of the disease process before overt pathology is recognizable. While the Ts16 mouse exhibits increased expression of the *App* gene and may also exhibit altered vascular permeability (18, 31), studies in Ts16 mice are limited at the moment to the prenatal period since Ts16 fetuses invariably die by birth.

This research was supported by Public Health Service Grants PO1 HD 19920 and RO1 HD 19932 and by the McKnight Foundation (J.T.C.). C.B. and G.L.F. are recipients of an European Economic Community Fellowship and are on leave of absence from the Instituto di Ricerche Farmacologiche 'Mario Negri' in Milano, Italy.

1. Glenner, G. G. & Wong, C. W. (1984) *Biochem. Biophys. Res. Commun.* **120**, 885–890.
2. Maters, C. L., Simms, G., Weinmann, N. A., Multhaup, G., McDonald, B. L. & Beyreuther, K. (1985) *Proc. Natl. Acad. Sci. USA* **82**, 4245–4249.
3. Coyle, J. T., Price, D. & DeLong, M. R. (1983) *Science* **219**, 1184–1190.
4. Wisniewski, K. E., Wisniewski, H. M. & Wen, G. Y. (1985) *Ann. Neurol.* **17**, 278–282.
5. Kang, J., Lemaire, H.-G., Unterbeck, A., Salbaum, J. M., Masters, C. L., Grzeschik, K. H., Multhaup, G., Beyreuther, K. & Muller-Hill, B. (1987) *Nature (London)* **325**, 733–736.
6. Robakis, N. K., Ramakrishna, N., Wolfe, G. & Wisniewski, H. M. (1987) *Proc. Natl. Acad. Sci. USA* **84**, 4190–4194.
7. Goldgaber, D., Lerman, M. I., McBride, W. O., Saffiotti, U. & Gajdusek, D. C. (1987) *Science* **235**, 877–880.
8. Coyle, J. T., Oster-Granite, M. L. & Gearhart, J. D. (1986) *Brain Res. Bull.* **16**, 773–787.
9. Scott, B. L., Becker, L. E. & Petit, T. L. (1985) *Prog. Neurobiol.* **21**, 199–237.
10. Reeves, R. H., Gearhart, J. D. & Littlefield, J. W. (1986) *Brain Res. Bull.* **16**, 803–814.
11. Cox, D. R. & Epstein, C. J. (1985) *Ann. N.Y. Acad. Sci.* **450**, 169–178.
12. Reeves, R. H., Robakis, N. K., Oster-Granite, M. L., Wisniewski, H. M., Coyle, J. T. & Gearhart, J. D. (1987) *Mol. Brain Res.* **2**, 215–221.
13. Lovett, M., Goldgaber, D., Ashley, P., Cox, D. R., Gajdusek, D. C. & Epstein, C. J. (1987) *Biochem. Biophys. Res. Commun.* **144**, 1069–1075.
14. Oster-Granite, M. L. (1986) *Brain Res. Bull.* **16**, 767–771.
15. Delabar, J. M., Goldgaber, D., Lauron, Y., Nicole, A., Huret, J. L., De-Grouchy, J., Brown, P., Gajdusek, D. C. & Sinet, P. M. (1987) *Science* **235**, 1390–1392.
16. Coyle, J. T. & Schwarcz, R. (1983) in *Handbook of Chemical Neuroanatomy*, eds. Bjorklund, L. & Hokfelt, T. (Elsevier, North Holland), Vol. 1, pp. 508–527.
17. Consolo, S., Wang, J.-X., Fusi, R., Vinci, R., Forloni, G. L. & Ladinsky, H. (1984) *Brain Res.* **303**, 147–151.
18. Gearhart, J. D., Davisson, M. T. & Oster-Granite, M. L. (1986) *Brain Res. Bull.* **16**, 789–801.
19. Eicher, E. M. & Washburn, L. L. (1978) *Proc. Natl. Acad. Sci. USA* **75**, 946–950.
20. Reeves, R. H., Morgan, R., Bendotti, C., Oster-Granite, M. L., Gearhart, J. D. & Coyle, J. T. (1987) *Soc. Neurosci. Abstr.* **13**, 1022.
21. Feinberg, P. & Vogelstein, B. (1984) *Anal. Biochem.* **137**, 266–267.
22. Young, W. S., III (1986) *Neuropeptides* **8**, 93–97.
23. Chirgwin, J. W., Przybyla, A. E., MacDonald, R. J. & Rutter, W. J. (1979) *Biochemistry* **18**, 5294–5299.
24. Thomas, P. (1980) *Proc. Natl. Acad. Sci. USA* **77**, 5201–5204.
25. Church, G. M. & Gilbert, W. (1984) *Proc. Natl. Acad. Sci. USA* **81**, 1991–1995.
26. Melton, D. A., Krieg, P. A., Rebagliati, T., Maniatis, T., Zinn, K. & Green, M. R. (1984) *Nucleic Acids Res.* **12**, 7035–7056.
27. Saltarelli, M. D., Forloni, G.-L., Oster-Granite, M. L., Gearhart, J. D. & Coyle, J. T. (1987) *Dev. Genet.* **8**, 267–279.
28. Bahmanyar, S., Higgins, G. A., Goldgaber, D., Lewis, D. A., Morrison, J. H., Wilson, M. C., Shankar, S. K. & Gajdusek, D. C. (1987) *Science* **237**, 77–80.
29. Tanzi, R. E., Gusella, J. F., Watkins, P. C., Bruns, G. A. P., St. George-Hysslop, P., Van Keuren, M. L., Patterson, D., Pagan, S., Kurnit, D. M. & Neve, R. L. (1987) *Science* **235**, 880–884.
30. Gearhart, J. D., Oster-Granite, M. L., Reeves, R. H. & Coyle, J. T. (1987) *Dev. Genet.* **8**, 249–265.
31. Kornguth, S. E., Bersu, E. T., Auerbach, R., Sobkowicz, H. M., Schutta, H. S. & Scott, G. L. (1986) *Ann. N.Y. Acad. Sci.* **477**, 160–178.